

Figure 3. Calculated bandwidths W_b' and W_b of $(\text{TMTSF})_2\text{X}$ along the interchain direction plotted as a function of the experimental interchain Se...Se separation, $d_{av} = (d_9 + 2d_7)/3$: (a) W_b' vs. d_{av} , and (b) W_b vs. d_{av} , where the values of W_b' and W_b are given in meV and the value of d_{av} is in Å. The empty and filled circles refer to the data for the 298 K and the 120–125 K structures, respectively. The numbers 1–8 represent the anions X^- of $(\text{TMTSF})_2\text{X}$ as follows: 1 = AsF_6^- , 2 = BF_4^- , 3 = BrO_4^- , 4 = ClO_4^- , 5 = FSO_3^- , 6 = H_2F_3^- , 7 = PF_6^- , and 8 = ReO_4^- .

with the magnitude of the interchain Se...Se interaction. The structural parameters relevant for describing the interchain Se...Se interactions are the two shortest interchain Se...Se separations d_9 and d_7 (see Figure 1 of ref 2). Between neighboring chains of TMTSF molecules, there occur one d_9 and two d_7 Se...Se contacts per TMTSF molecule. Since the Se 4p orbitals in the HOMO of each TMTSF have the same sign, all the Se 4p orbitals associated with the d_9 and d_7 Se...Se contacts can be chosen to have the same sign. Consequently, the weighted average of the interchain Se...Se separations $d_{av} = (d_9 + 2d_7)/3$ is a good experimental parameter to correlate with the calculated W_b' and W_b values. The plot of W_b' vs. d_{av} and that of W_b vs. d_{av} are respectively shown in Figure 3, which reveals that the lower band becomes wider but the upper band becomes narrower upon decreasing the interchain Se...Se separation.¹² Thus the magnitude of the interchain Se...Se interaction increases with the decrease in the interchain Se...Se separation according to the lower band, while the opposite is the case according to the upper band.

Figure 3 shows that, regardless of the temperature change, the data points for $\text{X}^- = \text{BF}_4^-$, ClO_4^- , and FSO_3^- are clearly separated out from those for $\text{X}^- = \text{AsF}_6^-$ and PF_6^- . Such a feature is also obtained when the unit cell volumes of $(\text{TMTSF})_2\text{X}$ are plotted against the d_{av} values.² Along the interchain direction, the upper (lower) bands of the BF_4^- , ClO_4^- , and FSO_3^- derivatives are narrower (wider) than the corresponding ones of the AsF_6^- and PF_6^- derivatives. Thus for the BF_4^- , ClO_4^- and FSO_3^- derivatives, it is expected that the density of states at the Fermi level is greater, the two sheets of the Fermi surface (see Figure 2a of ref 6) are less curved, but the overall interchain Se...Se interaction is stronger.¹³ A high transition temperature T_c for superconductivity is likely to occur from a nearly half-filled narrow band.¹⁴ However, such a band is also susceptible to electron localization.¹⁵ The competition between superconductivity and electron locali-

zation is quite delicate. For example, $(\text{TMTSF})_2\text{PF}_6$ undergoes a spin density wave (SDW) transition near 12 K at ambient pressure,¹⁶ while an applied pressure of about 12 kbar suppresses this SDW transition and gives rise to superconductivity.¹⁷ Thus it appears that under applied pressure the interchain Se...Se separations of $(\text{TMTSF})_2\text{PF}_6$ become shortened and close to those of $(\text{TMTSF})_2\text{ClO}_4$, a superconductor below 1.2 K at ambient pressure.^{4b}

In summary, characterization of the interchain Se...Se interaction in $(\text{TMTSF})_2\text{X}$ requires at least two parameters, e.g., the interchain bandwidths of the two overlapping bands that arise from the two TMTSF HOMO's of each unit cell. The magnitudes of the interchain Se...Se interaction predicted from the widths of those two bands exhibit the opposite trends with respect to the change in the interchain Se...Se separations. This kind of complex behavior of the interchain Se...Se interaction might be responsible for the wealth of physical phenomena observed in $(\text{TMTSF})_2\text{X}$.¹⁸

Acknowledgment. The work at North Carolina State University was supported by the Camille and Henry Dreyfus Foundation through a Teacher-Scholar Award to M.-H. W. The work at Argonne National Laboratory was supported by the U.S. Department of Energy, Office of Basic Energy Science, Division of Materials Science, under Contract W-31-109-Eng-38. We are thankful to Dr. P.M. Grant for communicating his work prior to publication.

Registry No. $(\text{TMTSF})_2\text{AF}_6$, 73731-75-6; $(\text{TMTSF})_2\text{BF}_4$, 73731-79-0; $(\text{TMTSF})_2\text{BrO}_4$, 81259-81-6; $(\text{TMTSF})_2\text{ClO}_4$, 72773-54-2; $(\text{TMTSF})_2\text{FSO}_3$, 81259-79-2; $(\text{TMTSF})_2\text{H}_2\text{F}_3$, 82979-12-2; $(\text{TMTSF})_2\text{PF}_6$, 73261-24-2; $(\text{TMTSF})_2\text{ReO}_4$, 80531-49-3; Se, 22541-48-6.

(16) (a) Bechgaard, K.; Jacobsen, C. S.; Mortensen, K.; Pedersen, H. J.; Thorup, N. *Solid State Commun.* **1980**, *33*, 1119. (b) Walsh, W. M., Jr.; Wudl, F.; Thomas, G. A.; Nalewajek, D.; Hauser, J. J.; Lee, P. A.; Poehler, T. *Phys. Rev. Lett.* **1980**, *45*, 829. (c) Scott, J. C.; Pedersen, H. J.; Bechgaard, K. *Phys. Rev. Lett.* **1980**, *45*, 2125. (d) Chaikin, P. M.; Grunner, G.; Engler, E. M.; Greene, R. L. *Phys. Rev. Lett.* **1980**, *45*, 1874. (e) Chaikin, P. M.; Tiedje, T.; Bloch, A. N. *Solid State Commun.* **1982**, *41*, 739.

(17) (a) Jerome, D.; Mazaud, A.; Ribault, M.; Bechgaard, K. *J. Phys. Lett. (Paris)* **1980**, *41*, L95. (b) Andres, K.; Wudl, F.; McWhan, D. B.; Thomas, G. A.; Nalewajek, K.; Stevens, A. L. *Phys. Rev. Lett.* **1980**, *45*, 1449.

(18) A recent summary of experimental and theoretical results on $(\text{TMTSF})_2\text{X}$ salts is found in *Mol. Cryst. Liq. Cryst.* **1982**, *79*, 1-359.

Bacteriorhodopsins Containing Cyanine Dye Chromophores. Support for the External Point-Charge Model

Fadila Derguini, Charles G. Caldwell, Michael G. Motto, Valeria Balogh-Nair, and Koji Nakanishi*

Department of Chemistry, Columbia University
New York, New York 10027

Received October 6, 1982

Bacteriorhodopsin¹ (bR, MW ~27 000), the protein pigment of the purple membrane of *Halobacterium halobium*, functions as a light-driven proton pump.² Its single polypeptide chain,^{3,4} which constitutes seven α -helical rods perpendicular to the membrane plane,⁵ is bound through lysine-216⁶⁻⁸ to *trans*-retinal

(12) The straight lines of Figure 3 may be used to approximate the relationship between W_b' and d_{av} and that between W_b and d_{av} , respectively. With W_b' and W_b in meV and d_{av} in Å, the linear equations are given as follows: $W_b' \approx -180d_{av} + 746$; $W_b \approx 167d_{av} - 608$. At 298 (120–125) K the intrachain bandwidths W_a of $(\text{TMTSF})_2\text{X}$ calculated without Se 4d orbitals are 0.463 (0.517), 0.449 (0.499), 0.446 (0.484), 0.452 (0.482), 0.448 (0.480), 0.522 (0.586), 0.463 (0.517), and 0.453 (0.497) eV for $\text{X}^- = \text{AsF}_6^-$, BF_4^- , BrO_4^- , ClO_4^- , FSO_3^- , H_2F_3^- , PF_6^- , and ReO_4^- , respectively.

(13) The upper (lower) band of Figure 1 is half (completely) filled. Thus the property representing all the electrons of the valence band is more influenced by the lower band.

(14) Krüger, E. *Phys. Status Solidi B* **1978**, *85*, 493.

(15) (a) Brandow, B. H. *Adv. Phys.* **1977**, *26*, 651. (b) Mott, N. F. "Metal-Insulator Transitions"; Barnes & Noble: New York, 1977. (c) Haas, C. "Current Topics in Materials Science"; Kaldis, E., Ed.; North-Holland: Amsterdam, 1979; Chapter 1. (d) Whangbo, M.-H. *Acc. Chem. Res.*, in press.

(1) Oesterhelt, D.; Stoekenius, W. *Nature (London) New Biol.* **1971**, *233*, 149-152.

(2) Oesterhelt, D.; Stoekenius, W. *Proc. Natl. Acad. Sci. U.S.A.* **1973**, *70*, 2853-2857.

(3) Ovchinnikov, Yu. A.; Abdulaev, N. G.; Feigina, M. Yu.; Kiselev, A. V.; Lobanov, N. A. *FEBS Lett.* **1979**, *100*, 219-224.

(4) Khorana, H. G.; Gerber, G. E.; Herlihy, W. C.; Gray, C. P.; Anderegg, R. J.; Nihei, K.; Biemann, K. *Proc. Natl. Acad. Sci. U.S.A.* **1979**, *76*, 5046-5050.

(5) Unwin, P. N. T.; Henderson, R. *Nature (London)* **1975**, *257*, 28-32.

(6) Bayley, H.; Huang, K. S.; Radhakrishnan, R.; Ross, A. H.; Takagaki, Y.; Khorana, H. G. *Proc. Natl. Acad. Sci. U.S.A.* **1981**, *78*, 2225-2229.

(7) Lemke, H.-D.; Oesterhelt, D. *FEBS Lett.* **1981**, *128*, 255-260.

(8) Mullen, E.; Johnson, A. H.; Akhtar, M. *FEBS Lett.* **1981**, *130*, 187-193.

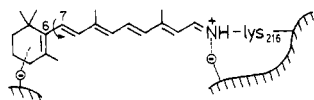
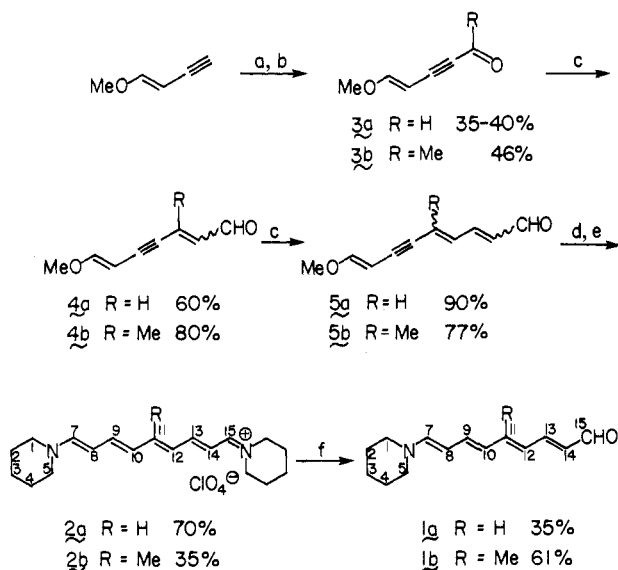


Figure 1. External point-charge model for bR.¹² In addition to the counteranion near the protonated nitrogen, a second charge is located near the ring. The ring-chain angle was arbitrarily set at 45°, but this angle has no bearing on the model.

Scheme I



^a (i) EtMgBr/THF/Et₂O/40–45 °C; (ii) RCHO (45–50 °C, 1 h for paraformaldehyde; 5–10 °C, 30 min for CH₃CHO). ^b MnO₂/Me₂CO/25 °C, 2–3 h. ^c Me₃SiCH₂CH=N-*t*-Bu/LDA/THF/–78 to 0 °C. ^d (i) H₂/Pd(CaCO₃, Pb poison)¹⁷/quinoline/EtOH; (ii) piperidine (1.1 equiv)/piperidinium perchlorate (1 equiv)/0 °C. ^e NaOH/H₂O/*N*-methylpyrrolidinone or CH₃CN.

via a protonated Schiff base (SBH⁺) linkage.^{9–11} Although the SBH⁺ of retinal with *n*-BuNH₂ absorbs at 440 nm (in MeOH), the maxima of light-adapted (LA) and dark-adapted (DA) bR appear at 570 and 560 nm, respectively. In order to account for these large spectral differences, we had proposed the external point-charge model (Figure 1) in which a point charge near the β-ionone ring assists in delocalizing the distribution of positive charge along the polyene chromophore.^{12,13}

Binding studies were carried out with merocyanines **1** (Scheme I) for the following reason. The iminium salts of merocyanines are cyanine dyes **2** in which the charge distribution is symmetric. If this symmetric cyanine dye structure of the chromophore could be ascertained in the pigment, it would furnish strong support for the model shown in Figure 1; it would also provide independent evidence for the SBH⁺ linkage,^{9,10} which was disputed by some workers until the recent FT IR studies.¹¹ These expectations have been fulfilled as described in this communication.

The syntheses of merocyanines **1** were closely related to those of similar compounds.¹⁴ The approach thus focused on the synthesis of the appropriate unsaturated side chains **5**, their hydrogenation and condensation with piperidine to give cyanines **2**, and finally hydrolysis to yield merocyanines **1**. While the un-

Table I. UV (nm) and CD Data of **1a**, **1b**, and Pigments Derived Therefrom

	1a	1b
(i) –CHO ^a	477 (ε 61 000), W _{1/2} 5100 ^g	475 (ε 74 000), W _{1/2} 5500 ^g
(ii) –C=N ⁺ H-Bu ^b	606, W _{1/2} 1300 ^g	623, W _{1/2} 1490 ^g
(iii) –C=N ⁺ -pip ^c	616 (ε 260 000), W _{1/2} 1200 ^g	637 (ε 250 000), W _{1/2} 1100 ^g
(iv) bR ^d	662, W _{1/2} 1350 ^g	662, W _{1/2} 1190 ^g
(v) OS ^e	1400 cm ⁻¹	950 cm ⁻¹
(vi) CD ^f	640(+)/680(-)	635(+)/670(-)

^a Merocyanines **1a** and **1b**, in MeOH. ^b SBH⁺ of *n*-butylamine, in MeOH. ^c Iminium salts **2a** and **2b**, in MeOH (pip = piperidine). ^d In 10 mM HEPES, pH 7.0. ^e Difference in λ_{max} (in cm⁻¹) between ii and iv.¹² ^f Wavelength and signs of Cotton effects, in 10 mM HEPES, pH 7.0. ^g Half-bandwidth in cm⁻¹.

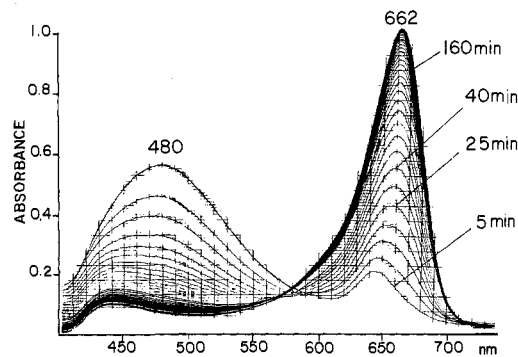


Figure 2. Absorption spectra obtained during the incubation of 11-methyl merocyanine **1b** with bleached purple membrane, in 10 mM HEPES buffer, pH 7, dark, 22 °C.

substituted side chain **5a** is available by the method of Malhotra and Whiting,¹⁴ an alternative route (see Scheme I) proved to be convenient for both **5a** and **5b**. Reaction of (*E*)-1-methoxy-1-buten-3-yne with ethylmagnesium bromide followed by treatment with solid paraformaldehyde and MnO₂ oxidation gave the aldehyde **3a**.¹⁵ The corresponding reaction sequence with (*E*)-1-methoxy-1-buten-3-yne and acetaldehyde provided ketone **3b**.¹⁵ Successive two-carbon elongations (with intermediate purification by flash column chromatography) using the silyl aldimine reagent¹⁶ then furnished the complete aldehyde side chains **5** as mixtures of configurational isomers.

Selective hydrogenation of the acetylenic linkage of **5a** was carried out as described previously.^{14,17} The crude product was condensed with piperidine and piperidinium perchlorate in ethanol, resulting in precipitation of **2a** as deep blue crystals [mp (EtOH) 154–155 °C,¹⁸ UV (MeOH) 616 nm (Table I)], the symmetric structure being fully supported by NMR data.^{19,20} Base treatment¹⁴ of **2a** yielded merocyanine **1a** [mp (EtOH) 173–174 °C, UV (MeOH) 477 nm].²¹ The corresponding sequence with

(15) Aldehyde **3a** (bp 52–55 °C (0.25 mmHg)) and ketone **3b** (bp 48–55 °C (0.15 mmHg)) were purified by distillation.

(16) Corey, E. J.; Enders, D.; Bock, M. G. *Tetrahedron Lett.* **1976**, 7–9.

(17) The Pd/CaCO₃ catalyst with lead poison is available from Aldrich Chemical Co.

(18) The configurational isomers of yne-trienals **5** are presumably converted into the all-trans-form **6** during this reaction.

(19) **2a**: ¹H NMR (CD₃OD, 250 MHz) δ 1.76 (m, 2,3(4)-H), 3.60 (m, 1(5)-H), 5.96 (t, *J* = 12 Hz, 8(14)-H), 6.23 (t, *J* = 12 Hz, 10(12)-H), 7.17 (t, *J* = 12 Hz, 11-H), 7.25 (t, *J* = 12 Hz, 9(13)-H), 7.45 (d, *J* = 12 Hz, 7(15)-H).

(20) Scheibe, G.; Seiffert, W.; Wengenmayr, H.; Jutz, C. *Ber. Bunsenges. Phys. Chem.* **1963**, 67, 560–570.

(21) **1a**: ¹H NMR (CD₃CN, 250 MHz) δ 1.52 (m, 2,3(4)-H), 3.12 (m, 1(5)-H), 5.29 (dd, *J* = 13 Hz, 11 Hz, 8-H), 5.92 (dd, *J* = 15 Hz, 8 Hz, 14-H), 5.95 (dd, *J* = 14 Hz, 11 Hz, 10-H), 6.19 (dd, *J* = 14 Hz, 11 Hz, 12-H), 6.55 (d, *J* = 13 Hz, 7-H), 6.57 (dd, *J* = 14 Hz, 11 Hz, 9-H), 6.78 (dd, *J* = 14 Hz, 11 Hz, 11-H), 7.21 (dd, *J* = 15 Hz, 11 Hz, 13-H), 9.41 (d, *J* = 8 Hz, 15-H).

(9) Lewis, A.; Spoonhower, J.; Bogomolni, R. A.; Lozier, R. H.; Stoeklenius, W. *Proc. Natl. Acad. Sci. U.S.A.* **1974**, 71, 4462–4466.

(10) Aton, B.; Doukas, A. G.; Callender, R. H.; Becher, B.; Ebrey, T. G. *Biochemistry* **1977**, 16, 2995–2999.

(11) FT IR studies have confirmed earlier resonance Raman spectroscopy results: (a) Rothschild, K. J.; Marrero, H. *Proc. Natl. Acad. Sci. U.S.A.* **1982**, 79, 4045–4049. (b) Bagley, K.; Dollinger, G.; Eisenstein, L.; Singh, A. K.; Zimanyi, L. *Ibid.* **1982**, 79, 4972.

(12) Nakanishi, K.; Balogh-Nair, V.; Arnaboldi, M.; Tsujimoto, K.; Honig, B. *J. Am. Chem. Soc.* **1980**, 102, 7945–7947.

(13) Motto, M. G.; Sheves, M.; Tsujimoto, K.; Balogh-Nair, V.; Nakanishi, K. *J. Am. Chem. Soc.* **1980**, 102, 7947–7949.

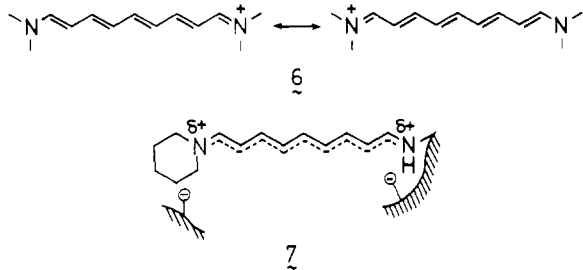
(14) Malhotra, S. S.; Whiting, M. C. *J. Chem. Soc.* **1960**, 3812–3822.

aldehyde **5b** yielded cyanine **2b** and merocyanine **1b**.²²

Purple membrane was isolated from *H. halobium* (strain R₁) according to Oesterhelt and Stoekenius.²³ Addition of retinal analogues **1a** and **1b**, solubilized in less than 2% EtOH, to bleached purple membrane suspensions in 10 mM or 50 mM HEPES, pH 7.0 at 22 °C, in the dark, resulted in the formation of bR analogues with absorption maxima at 662 nm (Figure 2 and Table I). Due to the lability of the chromophores in buffer, it was necessary to use a ca. 5-fold molar excess of chromophores to attain maximum regeneration yields of the pigments. The pigments were reasonably stable to 0.1 M NH₂OH at room temperature, i.e., there was less than 5% decrease of the 662-nm band in 5 h for the case of **1a** and in 2 h for the case of **1b**. The pigments thus formed were stable in the dark, only ca. 20% reduction in the 662-nm maxima being observed at 6 days at 22 °C. However, irradiation with light (>530 nm) at room temperature bleached 80% of the pigment from **1a** in 4 h and 90% of the methylated analogue within 40 min; shifts in the maxima of pigments, indicating formation of light-adapted species, could not be detected under these conditions.

It was not possible to apply the CH₂Cl₂ denaturation-extraction method²⁴ to check the integrity of the bound chromophore due to the instability of chromophores during the extraction procedure. The fact that chromophores **1a** and **1b** occupied the same binding site as *trans*-retinal was inferred from the following observations. The addition of *trans*-retinal to the maximally regenerated 662-nm pigments from **1a** and **1b** resulted in 38% and 52% growths, respectively, of the natural 560-nm peak. However, the 662-nm peak was not replaced by the 560-nm band, indicating that the retinal analogues were not displaced by *trans*-retinal. The biphasic nature of the CD curves (Table I) further supports occupation of the natural binding site.²⁵ The fact that these sites are not fully occupied by **1** is probably due to decomposition of the chromophore.²⁶ Further support that chromophores **1** were at the natural binding site was secured from the observation that no 662-nm pigment was formed upon addition of **1a** or **1b** to natural 560-nm bR (DA).

It is well established²⁷ that symmetric cyanines, exemplified by 9-(dimethylamino)nona-2,4,6,8-tetraenylidenedimethylammonium perchlorate **6**, λ_{max} (CH₂Cl₂) 625 nm (ε 295 000),¹⁴



have red-shifted absorption maxima characterized by narrow half-band widths ($W_{1/2}$) of ca. 1000 cm⁻¹. In contrast, in merocyanines having less uniform bond orders, the maxima are broad ($W_{1/2}$ ca. 6000 cm⁻¹) and blue-shifted. Note the broad and narrow

(22) Compounds **1b** and **2b** resisted crystallization. Merocyanine **1b** was purified by HPLC (Whatman Partisil ODS-2, 3% Et₃N in MeOH) immediately prior to binding experiments.

(23) Oesterhelt, D.; Stoekenius, W. *Methods Enzymol.* **1974**, *31*, 667-678.

(24) Pilkiewicz, F. G.; Pettei, M. J.; Yudd, A. P.; Nakanishi, K. *Exp. Eye Res.* **1977**, *24*, 421-423.

(25) In the case of purple membrane, the positive and negative CD bands (bR^{DA} 525(+)/595(-) and bR^{LA} 535(+)/602(-)) were interpreted as a result of exciton interaction between bacteriorhodopsin molecules within the trimers that form the rigid, hexagonal lattice of the membrane: Heyn, M. P.; Bauer, P. J.; Dencher, N. A. *Biochem. Biophys. Res. Commun.* **1975**, *67*, 897-903. Becher, B.; Cassim, J. Y. *Biophys. J.* **1976**, *16*, 1183-1200. Ebrey, T. G.; Becher, B.; Mao, B.; Kilbride, P. J. *Mol. Biol.* **1977**, *112*, 377-397.

(26) The 480-nm chromophore band diminishes with binding (Figure 2). However, this is accompanied by growth of maxima at 425 and 315 nm, most likely arising from decomposition of the chromophore during binding.

(27) Griffiths, J. "Colour and Constitution of Organic Molecules"; Academic Press: New York, 1976; p 244.

bandwidths, respectively, of unsymmetric merocyanines **1** and symmetric cyanines **2** (Table I, entries i and iii). The fact that the two bacteriorhodopsins derived from **1** have narrow bands absorbing at 662 nm provided excellent evidence for the symmetric cyanine dye structure **7** of the chromophore in these pigments, i.e., the data strongly support the external point-charge model as well as the SBH⁺ linkage shown in Figure 1. Theoretical calculations²⁸ fully corroborate these results. Preliminary experiments have also demonstrated that these cyanine pigments incorporated into vesicles lack the ability to translocate protons.

Acknowledgment. We are grateful to Drs. B. Honig, H. Kakitani, and T. Kakitani for discussions and to John D. Carriker for carrying out the binding studies. This work has been supported by NSF Grant CHE-8110505. C.G.C. was the recipient of an NIH postdoctoral fellowship award (F32GM07805).

Registry No. **1a**, 84215-22-5; **1b**, 84215-23-6; **2a**, 84215-25-8; **2b**, 84215-27-0; **3a**, 84215-28-1; **3b**, 84215-29-2; **4a**, 84215-30-5; **4b**, 84215-31-6; **5a**, 84215-32-7; **5b**, 84215-33-8; (*E*)-1-methoxy-1-buten-3-ene, 3685-20-9.

(28) Following paper in this issue.

Symmetric Charge Distribution in the Bacteriorhodopsin Binding Site

Toshiaki Kakitani,[†] Hiroko Kakitani,[†] and Barry Honig*

Department of Biochemistry, Columbia University
630 West 168th Street, New York, New York 10032

Koji Nakanishi

Department of Chemistry, Columbia University
New York, New York 10027

Received October 6, 1982

In the preceding paper¹ the synthesis of two merocyanine analogues of retinal was described. The binding of these compounds to bacteriorhodopsin results in the formation of stable pigments having narrow absorption maxima above 640 nm with half-bandwidths of approximately 1200 cm⁻¹. These observations were interpreted in terms of the formation of a cyanine dye within the bacteriorhodopsin binding site. In this communication we present theoretical calculations that strongly suggest that the protein-bound cyanine dye interacts with a symmetric distribution of electric charge. Consequently our results lend strong support for the "external point-charge" model for bacteriorhodopsin published previously.²

The red-shifted absorption maxima and narrow bandwidths (1000 cm⁻¹) of symmetric cyanine dyes result from their highly delocalized π electrons. In contrast, hydrocarbon polyenes, which have only limited π-electron delocalization (and hence significant bond alternation), exhibit broad absorption bands (6000 cm⁻¹) and short-wavelength absorption maxima. The width of electronic absorption bands is dependent upon the displacement of the equilibrium nuclear configuration in going from the ground to the excited state. Nonzero displacements lead to the appearance of symmetric vibrational progressions in the absorption spectrum (the Franck-Condon effect) and hence to a broadening of absorption bands. As the displacement increases, a longer progression is observed, and the band is increasingly broadened. Since in linear conjugated systems increased delocalization and hence reduced bond alternation is associated with reduced geometry changes upon excitation, symmetric cyanines have narrow bands while hydrocarbon polyenes have broad bands.³ Any perturbation that

[†] Present address: Department of Physics, Nagoya University, Chikusa-ku, Nagoya, 464, Japan.

(1) Derguini, F.; Caldwell, C.G.; Motto, M. G.; Balogh-Nair, V.; Nakanishi, K., preceding paper in this issue.

(2) Nakanishi, K.; Balogh-Nair, V.; Arnaboldi, M.; Tsujimoto, K.; Honig, B. *J. Am. Chem. Soc.* **1980**, *102*, 7945.